



Confronting cosmology and new physics with fundamental constants

Rodger I. Thompson

Steward Observatory – University of Arizona, Tucson, AZ 85721, USA
e-mail: rit@email.arizona.edu

Abstract. The values of the fundamental constants such as $\mu = m_p/m_e$, the proton to electron mass ratio and α , the fine structure constant, are sensitive to the product $\sqrt{\zeta_x^2(w+1)}$ where ζ_x is a coupling constant between a rolling scalar field responsible for the acceleration of the expansion of the universe and the electromagnetic field with x standing for either μ or α . The dark energy equation of state w can assume values different than -1 in cosmologies where the acceleration of the expansion is due to a scalar field. In this case the value of both μ and α changes with time. The values of the fundamental constants, therefore, monitor the equation of state and are a valuable tool for determining w as a function of redshift. In fact the rolling of the fundamental constants is one of the few definitive discriminators between acceleration due to a cosmological constant and acceleration due to a quintessence rolling scalar field. w is often given in parameterized form for comparison with observations. In this manuscript the predicted evolution of μ , is calculated for a range of parameterized equation of state models and compared to the observational constraints on $\Delta\mu/\mu$. We find that the current limits on $\Delta\mu/\mu$ place significant constraints on linear equation of state models and on thawing models where w deviates from -1 at late times. They also constrain non-dynamical models that have a constant w not equal to -1 . These constraints are an important complement to geometric tests of w in that geometric tests are sensitive to the evolution of the universe before the epoch of observation while fundamental constants are sensitive to the evolution of the universe after the observational epoch. Recent low redshift radio limits on $\Delta\mu/\mu$ provide the most significant constraints on the late time evolution of w .

Key words. (cosmology:) cosmological parameters – dark energy – theory – early universe

1. Introduction

The apparent acceleration of the expansion of the universe (Riess et al. 1998; Perlmutter et al. 1999) has spurred considerations of new physics and cosmologies beyond the standard model of physics and the Λ CDM cosmology. Since the fundamental constants such as the electromagnetic fine structure constant $\alpha = \frac{e^2}{\hbar c}$, the proton to electron mass ratio $\mu = \frac{m_p}{m_e}$ and

the gravitational fine structure constant $\frac{Gm_p m_e}{\hbar c}$ determine the quantitative nature of physics it is natural to check for time variations of these constants as an indicator of physics and cosmologies beyond the standard models. Rolling constants are one of the few definitive predictions of quintessence cosmologies that separate them from standard general relativity cosmological constant cosmologies.

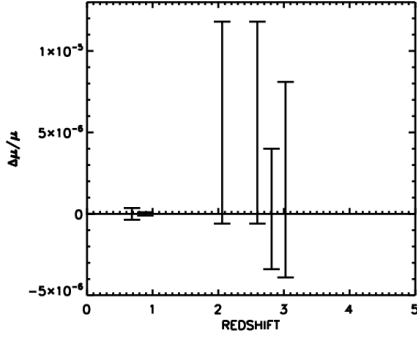


Fig. 1. Observational constraints on $\Delta\mu/\mu$ from radio ($z < 1$) and optical ($z > 1$) observations. All constraints are at the 1σ level except the radio constraint at $z = 0.6847$ which is 3σ . The radio constraint at $z = 0.8858$ is difficult to see at this scale but its value is $\pm 1 \times 10^{-7}$.

2. Observational constraints

The observational constraints on $\Delta\mu/\mu$ are shown in Figure 1 at the observed redshifts. Table 1 gives the redshifts, constraints, accuracy and references for the observations. At the scale of the figure the constraint at $z = 0.88582$ is difficult to see but its value is $\pm 1 \times 10^{-7}$. These constraints are the tightest published bounds for an object which may have several published constraints. The constraints at redshifts less than 1 are both radio observations while the remainder are from optical observations.

3. Relation between w and μ

The standard cosmology with a cosmological constant Λ predicts a very simple form of the dark energy equation of state, $w = -1$. Long standing difficulties in equating Λ with the particle physics vacuum energy (Weinberg 1989) has led to the consideration of other cosmologies with different values of w that can also evolve with time. Many of these cosmologies invoke a rolling scalar field ϕ that also couples with the electromagnetic field. For cosmologies where a single rolling scalar field couples with both the gravitational and electromagnetic fields Thompson (2012), utilizing the work of

Nunes & Lidsey (2004), Avelino et al. (2006) and Dutta & Scherrer (2011), showed that the change in μ is related to the EoS w and the coupling ζ_μ by

$$(w + 1)\zeta_\mu^2 = \frac{(\mu'/\mu)^2}{3\Omega_\phi} \quad (1)$$

where ' indicates the derivative with respect to the log of the scale factor a , $\ln(a)$. The evolution of μ is given by the integral

$$\frac{\Delta\mu}{\mu} = \zeta_\mu \int_1^a \sqrt{3\Omega_\phi(x)(w(x) + 1)} x^{-1} dx \quad (2)$$

which can be numerically integrated (Thompson 2012). When w is very close to -1 the ratio of the dark energy density to the critical density is well approximated by

$$\Omega_\phi = [1 + (\Omega_{\phi 0}^{-1} - 1)a^{-3}]^{-1} \quad (3)$$

When the value of w is significantly different than -1 , however, we use the more accurate form

$$\Omega_\phi(a) = [1 + (\Omega_{\phi 0}^{-1} - 1)a^{-3} \times \exp(3 \int_1^a \frac{(1 + w(x))}{3} dx)]^{-1} \quad (4)$$

For any given equation of state w we can then predict the change in μ as a function of the scale factor a under the assumption that w evolves due to a rolling scalar field that is coupled to μ with a coupling constant given by ζ_μ . Also note that both equation 1 and equation 2 indicate that *even a stationary value of w can cause μ to vary if the value is different from -1* . The same statement is true for α .

In this work we examine the evolution of μ for some common parameterizations of the EOS. As a benchmark we utilize a minimum expected value of ζ_μ of 4×10^{-6} . This value accepts the minimum expected value for ζ_α of 10^{-7} from Nunes & Lidsey (2004) multiplied by the expected ratio of $\Delta\mu/\mu$ to $\Delta\alpha/\alpha$ of 40-50 (Avelino et al. 2006). Note that the minimum ζ_α is calculated by assuming that the reported $\Delta\alpha/\alpha \approx 10^{-5}$ Webb et al. (2011) is real. If it is not then ζ_μ has no definite lower bound.

4. Equations of state

Several forms of the equation of state w are listed in DeFelice, Nesseris & Tsujikawa (2012), hereinafter DNT, which include the CPL or Chevallier-Polarski-Linder parameterization (Chevallier and Polarski 2001; Linder 2003)

$$w(a) = w_0 + w_1(1 - a) \quad (5)$$

where we also consider the case where $w_1 = 0$ for values of w_0 not equal to -1 .

DNT also consider three more parametrizations labeled Models 1 through 3. Here we only consider Model 1 where

$$w(a) = w_f + \frac{w_p - w_f}{1 + (a/a_t)^{1/\tau}} \quad (6)$$

where w_f is a future value of w , w_p is a past value of w , a is the scale parameter, a_t is a transition epoch and τ characterizes the transition time. For the purposes of this work Model 1 is considered general enough to represent most behaviors of w .

4.1. Constant and linear equations of state

From equation 2 it is obvious that the observed constraints on $\Delta\mu/\mu$ can be met for any EoS by simply lowering the value of ζ_μ . This frees up cosmological parameter space at the expense of further limiting the new physics parameter space. We will use our benchmark ζ_μ to evaluate the different EOS parameters with the full knowledge that it is based on the reported value of $\Delta\alpha/\alpha \approx 10^{-5}$

4.1.1. Constant EoS models

As noted at the end of Section 3 any deviation of w from -1 even if its value is constant will produce a time variation of μ . The magnitude of the variation depends on the range of the scale factors a where w deviates from -1 and the magnitude of the deviation. Constant EoS models are CPL models with $w_1 = 0$. We investigate four different constant EoS models, $w = -0.6, -0.8, -0.9, -0.999$. Figure 2 shows the evolution of $\Delta\mu/\mu$ for the constant EoS

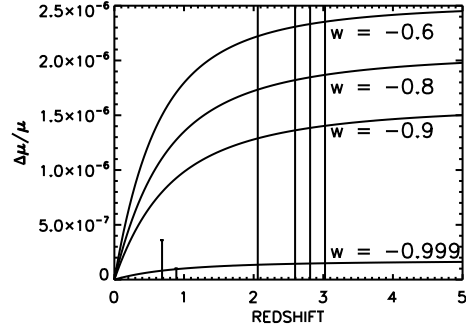


Fig. 2. Values of $\Delta\mu/\mu$ versus redshift for constant value EoS models with the values labeled in the plot. In this and subsequent plots we leave in the higher redshift constraints even though they are off scale just to show that they are met.

cases. Since these models have values of w different from -1 for all scale factors they show significant evolution of μ . Only the $w = -0.999$ case matches the low redshift $\Delta\mu/\mu$ constraints which indicates that most constant EoS models are highly disfavored. This is consistent with the previous work of Thompson (2013) that concluded that w must be within 0.001 of -1 between a redshift of 0.88582 and the present day, a time on the order of half of the age of the universe. Since we denote a change in μ as a difference between the value of μ at a given redshift and its value today a $\Delta\mu/\mu$ observation constrains the evolution of w between the scale factor of the observation and the scale factor now, taken to be 1. This is an example of how a non-geometrical test of the EoS can be very sensitive to models that would be difficult to discriminate against with a geometric test.

As an example Suzuki et al. (2012) used a combination of Hubble Space Telescope and ground based data to constrain the value of w based on type Ia Supernova, Baryonic Acoustic Oscillations, Cosmic Microwave Background, and Hubble Constant analysis. For the case of constant w they found $w = -1.006^{+0.110}_{-0.113}$ for $z < 0.5$ and $w = -0.69^{+0.80}_{-0.98}$ for $0.5 < z < 1.0$ combining both statistical and systematic errors. Strictly speaking these bounds are on the order of 100 less restrictive than the restriction of $w = -1^{+0.001}_{-0.001}$ found

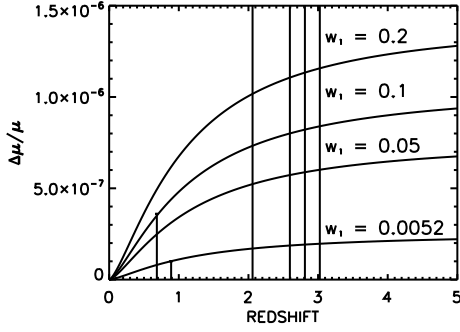


Fig. 3. Values of $\Delta\mu/\mu$ versus redshift for $w_0 = -1$ and varying w_1 . The values of w_1 are labeled in the plot.

here, however, this is based on a hard limit on $\zeta_\mu > 4.0 \times 10^{-6}$. At this point there is no appropriate statistical boundary on that limit.

4.1.2. Linear EoS models

For linear equations of state we use the simple equation 5 CPL formulation with just the two parameters, the current value of w , w_0 and the slope w_1 . In Section 4.1.1 we saw that only models with w_0 very close to -1 satisfied the constraints so in this section we set $w_0 = -1$ and vary the value of w_1 to test what range of linear models satisfy the $\Delta\mu/\mu$ constraints. We chose w_1 values of 0.2, 0.1, 0.05 and 0.0052 with the last value the only one that satisfies all of the constraints. Figure 3 shows the evolution of $\Delta\mu/\mu$. The net result is that only models with very shallow slopes ($w_1 < 0.0052$) and current EOS values very near -1 satisfy the observational constraints on $\Delta\mu/\mu$. We should note that all of the linear EOS models that have present day values of -1 and negative slopes in a are crossing the phantom divide, $w < -1$, at the present time. Those with positive slope have been in the phantom space at earlier times. It would appear that the parameter space for CPL equations of state is extremely limited other than the trivial case of $w = -1$.

Suzuki et al. (2012) also consider the case of the CPL linear model and find that $w_0 = -1.046^{+0.179}_{-0.170}$ and $w_1 = 0.14^{+0.60}_{-0.76}$. Again our formal results suggest a much tighter bound

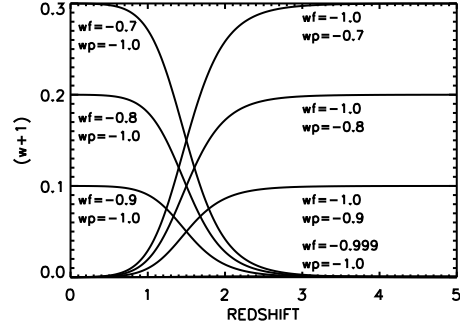


Fig. 4. Values of $(w + 1)$ versus redshift for Model 1 with the future, w_f , and past, w_p , values labeled on the plot. Note that the thawing model with $w = 0.999$ has a future $(w + 1)$ value of 0.001 which is not visible on the scale of this plot. All of the cases have $\tau = 0.1$ and $a_t = 0.4$.

on both w_0 and w_1 modulo the validity of the lower bound on the coupling constant ζ_μ .

4.2. Freezing and Thawing equations of state

Freezing equations of state start with an EOS different from -1 and approach -1 at the present time. Thawing equations of state start with an EOS very close to -1 and diverge from -1 at the present time. To investigate the differences between the two types of EOS forms we utilize Model 1 of DNT given by equation 6. The model has four parameters, w_p , the value of w in the past, w_f , the value of w in the future, τ , the transition time, and a_t the transition epoch. We chose a value of $\tau = 0.1$ to make the transition fast enough to define to regions with well defined asymptotic behavior. The transition epoch is chosen as $a_t = 0.4$ which corresponds to a redshift of $z = 1.5$. This produces a value of w very near -1 in the present epoch for freezing equations of state. Figure 4 shows the values of $(w+1)$ versus redshift for a range of values of w_p and w_f . In all of the cases we have set $\tau = 0.1$ and $a_t = 0.4$.

It is fairly easy to see how the plots in Figure 4 change as the parameters are varied. Varying the transition epoch a_t moves the tran-

Table 1. Observational constraints used in this analysis. References: (a) Wendt & Reimers (2008), (b) King et al. (2009), (c) King et al. (2011), (d) Malec et al. (2010), (e) Bagdonaitė et al. (2013), (f) Kanekar (2011)

Object	Redshift	$\Delta\mu/\mu$	error	Acc.	Ref.
Q0347-383	3.025	2.1×10^{-6}	$\pm 6. \times 10^{-6}$	1σ	(a)
Q0405-443	2.597	10.1×10^{-6}	$\pm 6.2 \times 10^{-6}$	1σ	(b)
Q0528-250	2.811	3.0×10^{-7}	$\pm 3.7 \times 10^{-6}$	1σ	(c)
J2123-005	2.059	5.6×10^{-6}	$\pm 6.2 \times 10^{-6}$	1σ	(d)
PKS1830-211	0.886	0.0	$\pm 1.0 \times 10^{-7}$	1σ	(e)
B0218+357	0.685	0.0	$\pm 3.6 \times 10^{-7}$	3σ	(f)

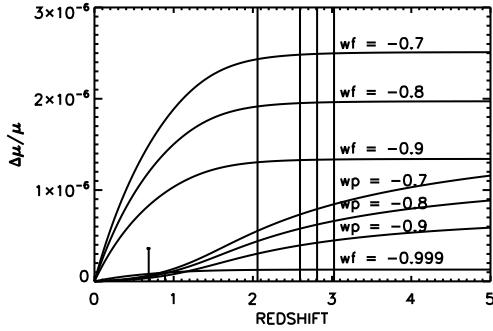


Fig. 5. Values of $\Delta\mu/\mu$ versus redshift for Model 1 with the future, wf , and past, wp , values labeled on the plot. The plots labeled with wf values are the thawing models shown in figure 4 and those labeled with wp values are the freezing models.

sition region along the redshift axis and varying the transition time τ changes the steepness of the transition.

We again use equation 2 and 4 to calculate the evolution of μ with redshift or scale factor. Figure 5 shows the evolution of μ for the parameters used in the EOS models shown in Fig. 4. The evolution of μ shown in Figure 5 follows the expected trajectories with thawing EoS models showing significantly more late time evolution due to their present day deviation from $w = -1$. Figure 6 shows that all of the freezing models either meet the constraint at $z = 0.88582$ or, in the case of $w_p = -0.7$, miss it by a very small amount. These models make it clear that the current much looser constraints at high redshift from the optical observations allow significant early time evolution

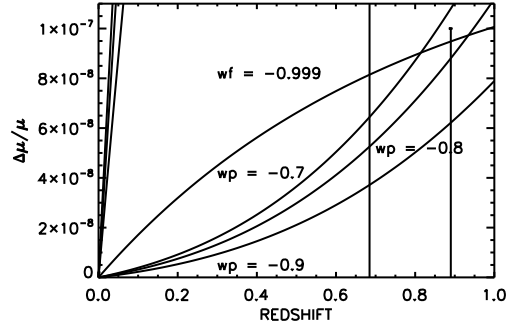


Fig. 6. This is an expanded view of the late time μ evolution shown in Figure 5 to show the detail of the $\Delta\mu/\mu$ near the most restrictive constraint at $z = 0.88582$.

of w as long as the value of w approaches -1 by a redshift of 1 or higher. We can say that thawing models with significant deviations from -1 are strongly disfavored. The looser constraints at high redshift can not put the same condition on freezing models. Consistent with the results from the linear EoS models the thawing model with a future value of $w = -0.999$ does meet the low redshift constraint.

5. Conclusions

For a given value of the coupling the deviation of μ or α depends on the amount of time, redshift or scale factor that w deviates from -1 . This feature strongly disfavors an EoS that has a constant value not equal to -1 as this maximizes the amount of time at a value of w other than -1 . The current limit on a constant w is

$w = -1 \pm 0.001$ at the 3σ level. This is essentially indistinguishable from -1 in geometric tests. Similarly linear or CPL models are also disfavored at a slightly lower level and are limited to slopes less than 0.005 for the case of $w_0 = -1$. Any value of w_0 other than -1 is further disfavored as the constant term also creates evolution of the constants.

The current data set places much more stringent constraints on thawing models than freezing models since fundamental constant tests constrain the evolution during the time between the observation and the present day unlike geometric tests that constrain the evolution that occurred before the observations. Since the most stringent constraints are for observations at $z < 1$ thawing models with significant late time evolution are particularly limited by the data. Freezing models with most of their evolution before the epoch of the observations are not as tightly constrained but it would not be correct to declare either model as more favored or disfavored but rather as less or more constrained. All of the model 1 freezing cases either satisfy or come very close to satisfying the constraints even with past EoSs quite deviant from -1 . The only thawing model 1 to pass the test had the its final value of w at $w = -0.999$ similar to the constant w case. However, moving the transition epoch to a later time would disqualify most of the freezing models.

Modulo the uncertainty on the true lower limit on $|\zeta_\mu|$ the range of possible EoS models is significantly constrained by the limits on the variation of μ . In particular the simple CPL linear EoS model has a very limited range of values which only accommodates slight deviations from -1 . At this point, except for the reported change in the value of α by Webb et al. (2011), the fundamental constant data are consistent with a cosmological constant and the standard model of physics. Higher accu-

racy measurements at high redshift will be particularly relevant for putting more significant limits on EoS models in general and on particular cosmological models.

Acknowledgements. The author would like to acknowledge very useful discussions with Carlos Martins on many aspects of the work present here as well as the many fruitful interactions during this conference.

References

- Avelino, P.P, Martins, C.J.A.P, Nunes, N.J., & Olive, K.A. 2006, Phys. Rev. D, 74, 083508
 Bagdonaite, J., et al. 2013, Science, 339, 46
 Chevallier, M., & Polarski, D. 2001, Int. J. Mod. Phys. D, 10, 213
 DeFelice, A., Nesseris, S., & Tsujikawa, S. 2012, JCAP, 5, 29
 Dutta, S., & Scherrer, R.J. 2011, Phys. Lett. B, 704, 265
 Kanekar, N. 2011, ApJ, 728, L12
 King, J. A., Webb, J. K., Murphy, M. T., & Carswell, R. F. 2009, Phys. Rev. Lett., 101, 251304
 King, J. A., et al. 2011, MNRAS, 417, 3010
 Linder, E.V. 2003, Phys. Rev. Lett., 90, 091301
 Malec, A.L., et al. 2010, MNRAS, 403, 1541
 Nunes, N.J., & Lidsey, J.E. 2004, Phys Rev D, 69, 123511
 Perlmutter, S., et al. 1999, ApJ, 517, 565
 Riess, A.G., et al. 1998, AJ, 116, 1009
 Salzano, V., Wang, Y., Sendra, I., & Lazkov, R. 2013, arXiv:1211.1012v2
 Suzuki, N., et al. 2012, ApJ, 746, 85
 Thompson, R.I. 2012, MNRAS Letters, 422, L67
 Thompson, R.I. 2013 MNRAS, 431, 2576
 Webb, J.K., et al. 2011, Phys. Rev. Lett., 107, 191101
 Weinberg, S. 1989, Rev. Mod. Phys. 61, 1
 Wendt, M., & Reimers, D. 2008, Eur. Phys. J-Spec. Top, 163, 197